

THE RELATIVITY GYROSCOPE EXPERIMENTS
AT STANFORD UNIVERSITY

W. STEPHEN CHEUNG

W. W. HANSEN LABORATORIES OF PHYSICS
STANFORD UNIVERSITY
STANFORD, CALIFORNIA 94305 U.S.A.

in

*Proceedings of the 1983 International School and Symposium on
Precision Measurement and Gravity Experiment, Taipei, Republic of
China, January 24 - February 2, 1983, ed. by W.-T. Ni (Published
by National Tsing Hua University, Hsinchu, Taiwan, Republic of
China, June, 1983)*

OUTLINE

I. Introduction	611
II. Description of the Experiment	614
III. The Gyroscope	614
IV. Rotor Coating	618
V. Gyro Housing	620
VI. Electric Suspension System	620
VII. Telescope	620
VIII. London Moment Readout	622
IX. Ultra Low Magnetic Field	622
X. Error Analysis	624
XI. Data Acquisition	627
XII. Electrical Breakdown Study	630
References	633

THE RELATIVITY GYROSCOPE EXPERIMENT AT STANFORD UNIVERSITY

W. Stephen Cheung
W.W. Hansen Laboratories of Physics
Stanford University, Stanford, CA 94305

I. Introduction

Einstein is generally regarded as the most eminent among scientists of this century. His special theory of relativity is tested and applied every day in various accelerators around the world. Except among workers in the field, Einstein's general theory of relativity is also believed to be the correct theory to replace the Newtonian version of gravity. People are told that measurements from three early experiments supported general relativity. These experiments are: a) the bending of starlight, b) perihelion of Mercury, and c) gravitational redshift. Moreover, people are told that general relativity has little everyday applications and that its effects are so few and so small that there is little hope and value to establish a field of experimental gravitation like the size of, say, solid state physics.

Since the birth of general relativity, there have been a number of viable theories proposed to compete with, if not to replace, general relativity. General relativity and a few of these theories passed the various conditions set to evaluate a viable theory of gravitation; this work was started by Dicke¹.

The parameter of special relativistic effects is v^2/c^2 and modern accelerators can push this parameter very close to unity. In the case of general relativity, the corresponding parameter is GM/rc^2 where M is the mass of the object generating the gravity field. This quantity is 10^{-9} on the surface of the Earth and 10^{-6} on the surface of the Sun. It is impossible to increase this parameter in our earthbound laboratories. Since this parameter is so small even for the Sun, general relativity, which is non-linear, can be linearized when calculating most effects in the solar system. Well known observations, except the advance of the perihelion of Mercury, only test the linearized theory.

With the advance in experimental techniques, measurement of general relativistic effects in the laboratory are now possible. The gravitational redshift measurement² performed at the Harvard Tower is one example. Today, there are over forty groups in the world searching for gravitational waves.

Except the perihelion of Mercury and the gyroscopic effects to be discussed below, all the other tests of general relativity employ radiation of some kind, be it gravitational or electromagnetic. Hence, there is a need to look for dynamic effects which are crucial in the understanding and the theoretical development of astrophysical objects such as black holes and pulsars. From the point of view of the experimentalists, there is also a need to refine past tests and to perform future tests with higher accuracy.

In 1960, Schiff³ suggested that a measurement of the precession of the spin axis of a perfect gyroscope orbiting about the Earth would provide a dynamic test of general relativity. Two main effects were predicted. The geodetic effect is due to the motion of the gyroscope about the earth's warped space-time and the corresponding drift rate Ω_G is given by

$$\Omega_G = \frac{3GM}{2c^2 R^3} (\vec{R} \times \vec{v}) \quad (1)$$

where \vec{R} and \vec{v} are the coordinate and velocity of the gyroscope and M is the mass of the earth.

The motional effect is due to the rotation of the earth and is given by

$$\Omega_M = \frac{GI}{c^2 R^3} \left\{ \frac{3\vec{R}}{r^2} (\vec{\omega} \cdot \vec{r}) - \vec{\omega} \right\} \quad (2)$$

where I and $\vec{\omega}$ are the moment of inertia and angular velocity of the earth.

Since the earth's rotation axis is not a good reference, the above drifts are with respect to an axis pointing at a fixed star. In a polar orbit, the two precession vectors, $\vec{\Omega}_G$ and $\vec{\Omega}_M$, are perpendicular to each other with $\vec{\Omega}_G$ perpendicular to the plane of the orbit and $\vec{\Omega}_M$ parallel to the Earth's axis. Fig.1 shows two gyroscopes in a polar orbit 500 miles above the earth and the precessions of these gyroscopes are as shown. The magnitude of Ω_G is about 7 arc-second and that of Ω_M is 0.05 arc-second after integrated over one year. Note that one arc-second is 4.8×10^{-6} radian.

Other viable theories, such as the scalar tensor theory of Brans and Dicke⁴, can also be tested by the results of these drifts if the resolution of the angular measurement is fine enough. The value of Ω_G predicted by the scalar-tensor theory is 6.3 arc-second/year. It therefore appears that an experiment with an accuracy of 0.1 arc-second/year would provide a clear test of general relativity and the scalar-tensor theory. However, such an accuracy would be insufficient to observe the motional effect which is of high interest to the verification of the frame dragging effect⁵. In fact, an accuracy of 1 milliarc-second/year would allow the measurement be done within 1 or 2%.

Analysis and experimental work on the gyroscope program, currently funded by the National Aeronautics and Space Administration (NASA) started at the Physics Department and the Department of Aeronautics and Astronautics of Stanford University in 1963. Clearly, the design of this experiment involves more than just two gyroscopes. In the next section, the proposed experiment will be described. Then, brief accounts on several areas will be given. It is, however, not the intention of this paper to cover each area extensively. Interested readers are referred to the specialized papers listed in the references. Also,

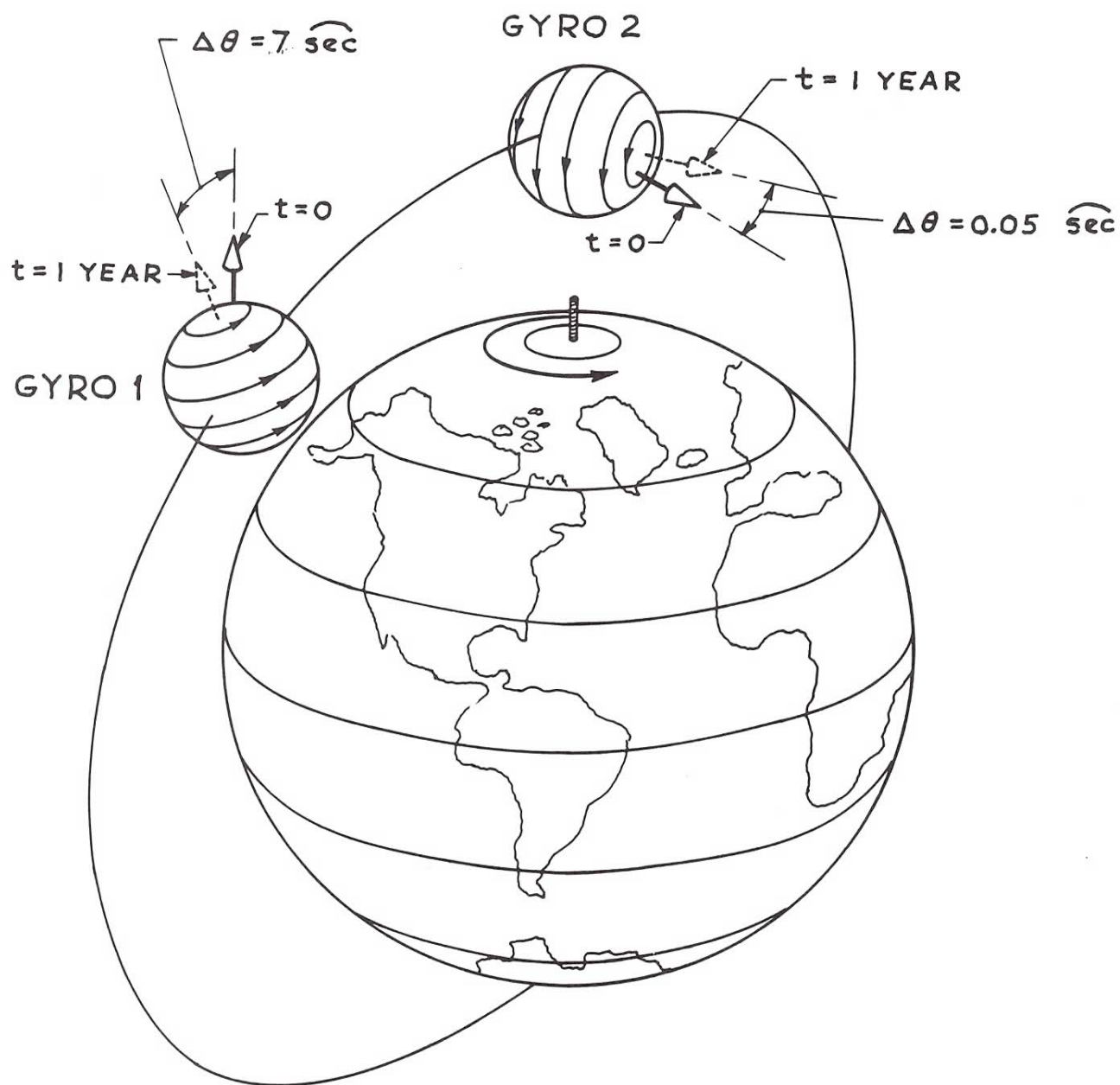


Figure 1: The relativistic effects of the earth on gyroscopes. Gyro 1 shows the geodetic effect and Gyro 2 shows the motional effect.

metric and English units are used in a somewhat mixed manner. A list of conversions is given below and the author apologizes to those who are inconvenienced.

$$1 \text{ arc-sec} = 4.8 \times 10^{-6} \text{ radian}$$

$$1 \text{ mil} = 10^{-3} \text{ inch}$$

$$1 \text{ } \mu\text{in} = 10^{-6} \text{ inch} = 250 \text{ } \text{\AA}$$

II. Description of the Experiment

The general view of the Relativity Gyroscope satellite is shown in Fig.2. Four quartz gyroscopes and a proof mass are housed inside a block of fused quartz. This block is optically contacted to a telescope which is also made of quartz. This quartz assembly is enclosed in a dewar vessel which contains several hundred litres of liquid helium at a temperature of 1.6°K .

The quartz gyro is a sphere 38 mm in diameter and coated with superconducting niobium of about $2500 \text{ } \text{\AA}$ thick. Each gyro is electrically suspended in an evacuated spherical cavity by voltages applied to three mutually perpendicular sets of electrodes. The electrodes are saucer-shaped and are metals deposited on the inside of the quartz cavity (Fig. 3A). After suspended, each gyro is spun up to about 170 Hz by gas jets passing through channels whose design is shown in Fig.3B. The gas is then exhausted and the cavity pressure will be kept at 10^{-9} torr. The characteristic spin down time of the gyro at 10^{-9} torr is about 400 years.

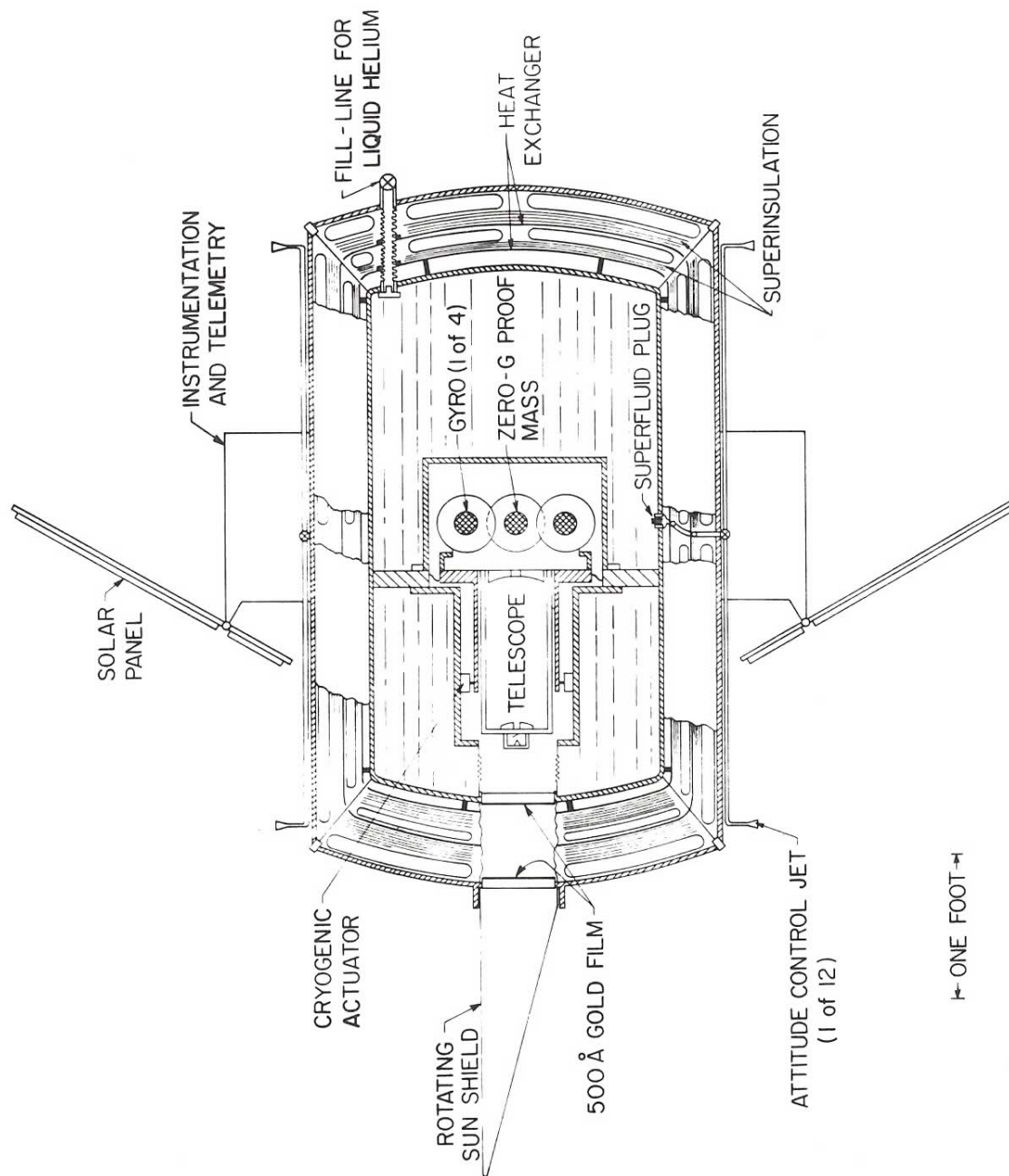
Operating the experiment at cryogenic temperatures allows us to exploit the special properties of superconductors to read out the direction of the gyro spin axis, to achieve an ultra low magnetic field environment, and to control the liquid helium flow inside the specially designed dewar.

The telescope points at a guide star, currently chosen to be Rigel, and the relativistic drifts of the gyros are compared to this line of sight. The boil-off helium gas is used to maneuver the spacecraft transversely to maintain this line of sight. It is also used in a drag free attitude control system that maintains the satellite in orbit with the average internal accelerations on the gyro from external drags and disturbances to about $10^{-10}g$ ($1g \approx 980 \text{ cm/sec}^2$).

The satellite is rolled about its line of sight to Rigel at a period of about 10 minutes. The telescope-gyro assembly is also made to dither with respect to this line of sight at about 0.1 Hz. The first is a synchronous detection scheme that helps single out relativistic signals from noise. The second motion is, in addition to synchronous detection, part of an inner control loop that maintains the line of sight with Rigel within a milliarc-second accuracy.

III. The Gyroscope

The size of the gyroscope was chosen in a somewhat arbitrary manner. The original gyro that came with the electric suspension system purchased



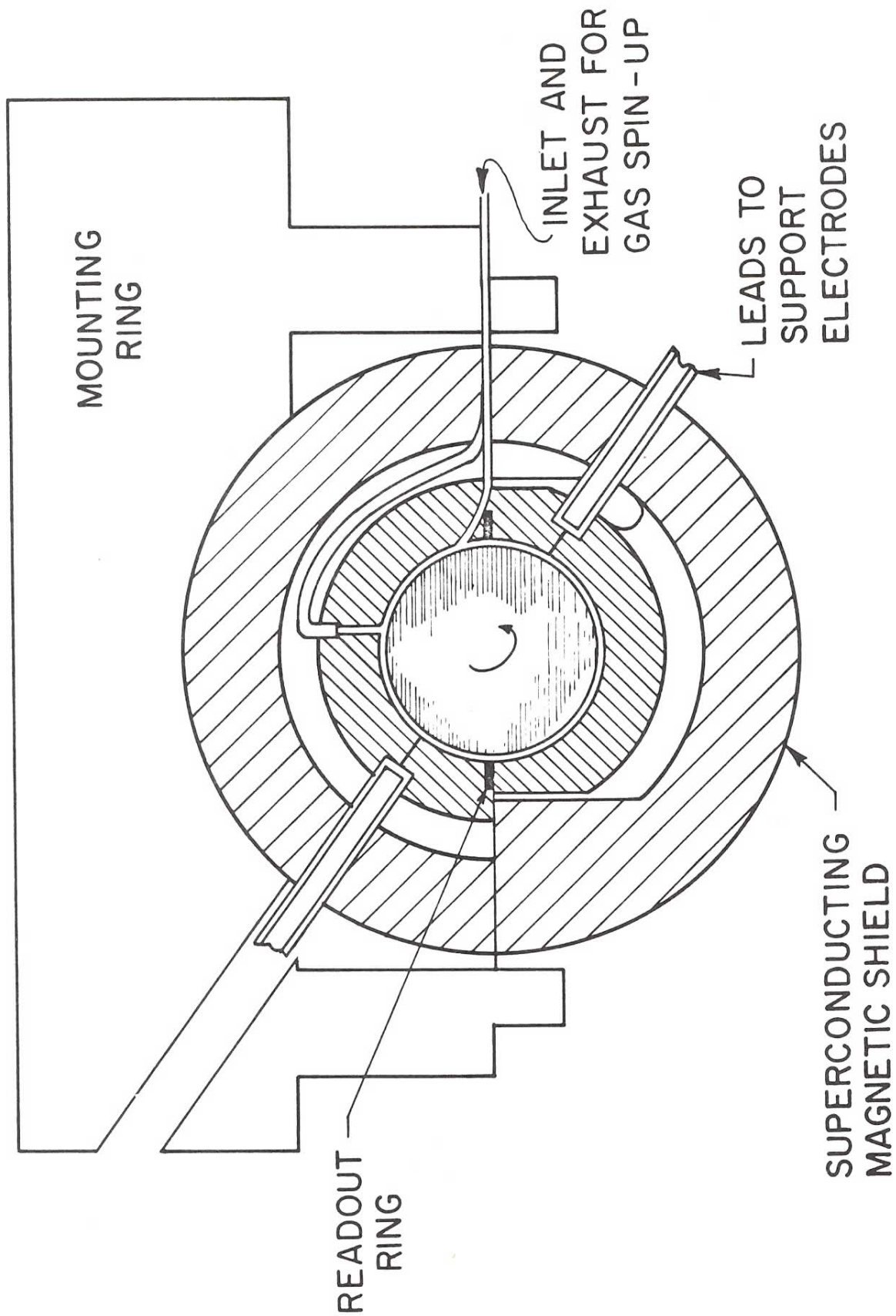


Figure 3A

Gyroscope Suspended Inside a Housing as a Laboratory Setup

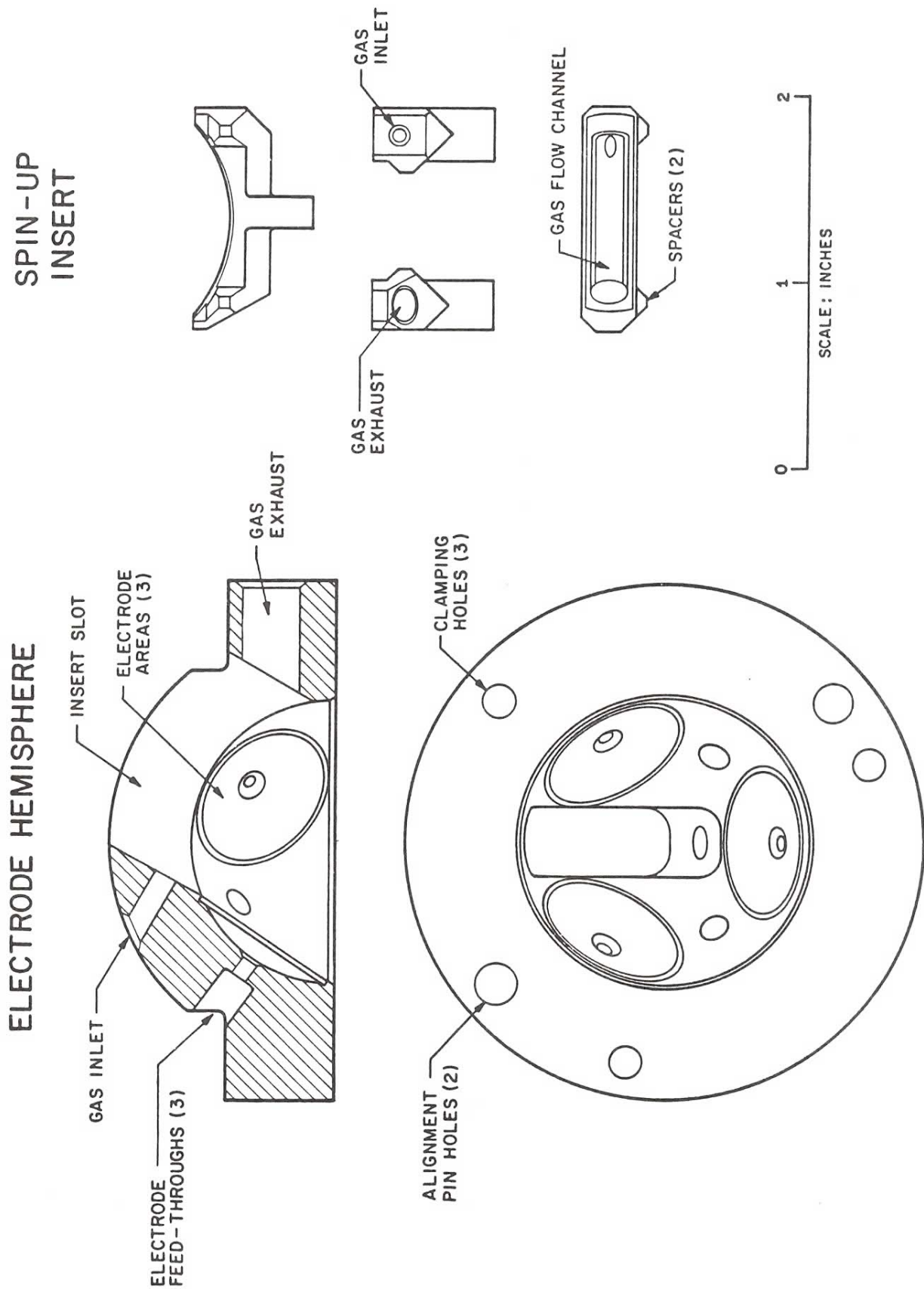


Figure 3B

from Honey-well was about this size. The gyro is made from optically selected fused quartz, homogeneous in density to a few parts in 10^7 and spherical to a fraction of a microinch (10^{-6} inch). Quartz is used because of its mechanical stability at cryogenic temperatures.

Mechanical stability is crucial in ensuring no distortion within the telescope-gyro structure whenever a heat flux passes through the structure perpendicular to the telescope axis causing differential thermal expansions to occur. If the heat flux from the solar radiation can be appropriately shielded, such hope is achievable because the coefficient of thermal expansion at cryogenic temperatures goes down by several orders.

That quartz is transparent allows the gyro's density homogeneity to be evaluated by measuring its optical index of refraction. The study by G. Siddall⁵ of Stanford of both theoretical and experimental work shows the relationship

$$\frac{\Delta\rho}{\rho} = 2.3 \frac{\Delta n}{n}$$

as a good empirical fit between variations in density and refractive index for a wide range of glasses.

The sphericity specification of the quartz gyro was unprecedented. To meet this challenge, a lapping machine was developed by W. Angele⁷ of NASA Marshall Flight Center (MFC) and the University of Alabama, Huntsville. The machine has four spherical laps arranged in a tetrahedral configuration. Each lap is driven at a different speed and at a different sense in a sequenced pattern to randomize the lapping process. As a result of this work, balls with peak-to-valley variations in sphericity near $0.1 \mu\text{in}$ can now be made.

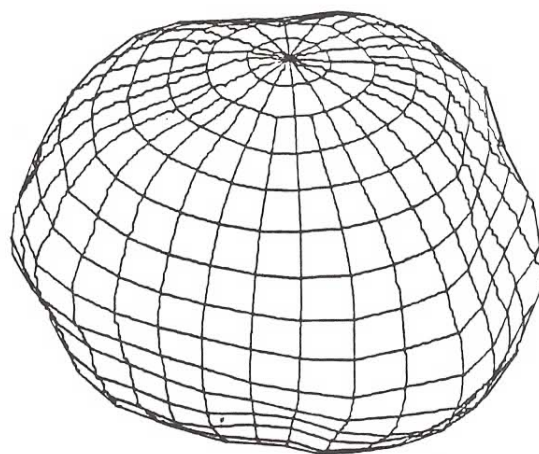
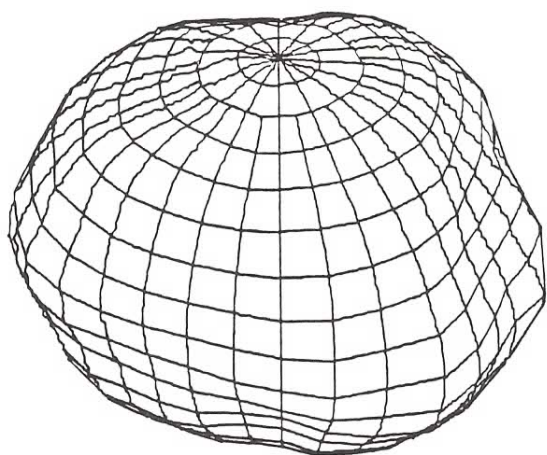
A ball of unprecedented roundness calls for a device to measure it. The roundness measurement is currently done by means of a Talynova II Roundness Measuring System developed by Rank, Taylor, Hobson Limited of Leicester, England. With the aid from a computer and error separation techniques, a precision of $0.1 \mu\text{in}$ in radius variation can be achieved. Fig.4 shows two stereoscopic pairs of surface maps at a magnification of 500,000.


IV. Rotor Coating

The superconductor coating on the gyro is for use in reading the instantaneous spinning axis of the gyro from its London Moment. London Moment will be discussed later.

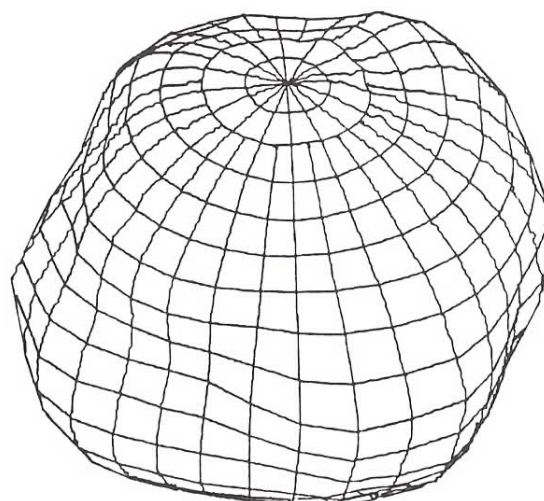
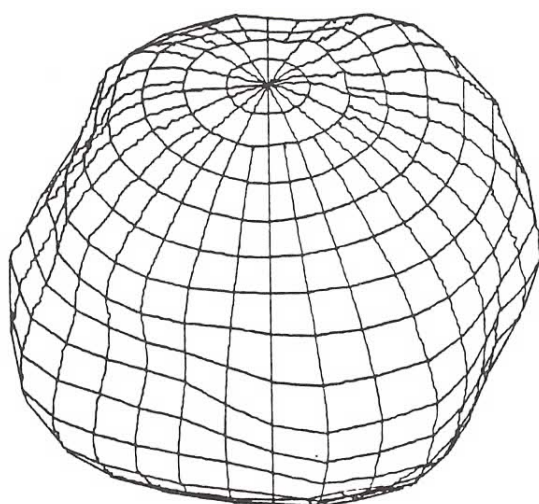
The superconductor coating is deposited on the gyro surface by means of sputtering. In order to have a uniform coating thickness, the ball should be turned to expose all parts of the surface equally during the sputtering process. A method developed by J. Lipa of Stanford is to use a mechanical ball tumbler controlled by a microcomputer. Another method by P. Peters of MFC is to tumble the ball inside the sputtering chamber with the ball floated on a stream of argon gas. The thickness uniformity is measured with a β -ray backscattering apparatus. At 1% uniformity, which appears to be achievable, a thickness over $10 \mu\text{in}$

FRONT VIEW



SCALE:  100 nanometers

BACK VIEW



SUPPRESSED RADIUS: 2 cm

STEREO VIEWS OF QUARTZ ROTOR

Figure 4

would upset the balance of the ball.

A coating of 30 \AA is enough to give a full London moment. Hence, a coating of 30 \AA is, in principle, all that is necessary. However, experiences at Stanford and at MFC have shown that severe arcing occurred causing failure in suspension when gyros of coating as thick as 10 \mu in were levitated. An ac voltage as high as 1.5 kV is necessary to levitate a quartz gyro (about 80 gm) on Earth but only a fraction of a volt in space. The problem of arcing and electrical breakdown will be dealt with later.

V. Gyro Housing

The quartz block in Fig.1 houses four gyroscopes and one proof mass. For laboratory testing purposes, single gyro housings have so far been designed and used. Gyro operations at room temperature and liquid helium temperatures are now studied extensively at Stanford and MFC.

Fig.3A shows the design of a single gyro housing with spin-up and pump-out channels. The housing is in two halves pinned together after the gyro has been put in place.

When suspended at the center position, the gap between the gyro surface and its opposing electrode is about 1.5 mil ($1 \text{ mil} = 10^{-3} \text{ inch}$). Six electrodes are sputtered on the housing as shown in Fig.3B. The sphericity requirement of the housing can be found in Table 1 which lists the rest of other requirements. Various experimental findings related to the gyro housing are discussed in reference 8.

VI. Electric Suspension System

Electric suspension was invented by A. Nordsieck of the University of Illinois in 1953 and has been further developed by several companies. Like magnetic suspension, it is a contactless levitation of an object against external accelerations, especially that of gravity, by means of electric fields. But an electric force is usually weaker than its magnetic counterpart; electric suspensions suffer from more practical limits than magnetic suspensions. The suspension gap must be small to reduce applied voltages and vacuum is invariably needed. Although initially thought of, magnetic suspension of the gyros was ruled out after the London moment readout scheme was conceived.

The gyro is levitated inside the cavity by three pairs of orthogonal electrodes. For each pair of electrodes, the position error signal of the gyro along that axis is capacitively sensed by a 1 MHz wave applied to each pair of electrodes. The error signal is then processed through a feedback network which regulates a 20 kHz voltage applied to the same electrode pair.

VII. Telescope

Fig.5 illustrates the general optical layout of the completed telescope. The optics is of the folded Schmidt-Cassegranian type, with 150 in. focal length and 5.6 in. aperture. The physical dimensions are:

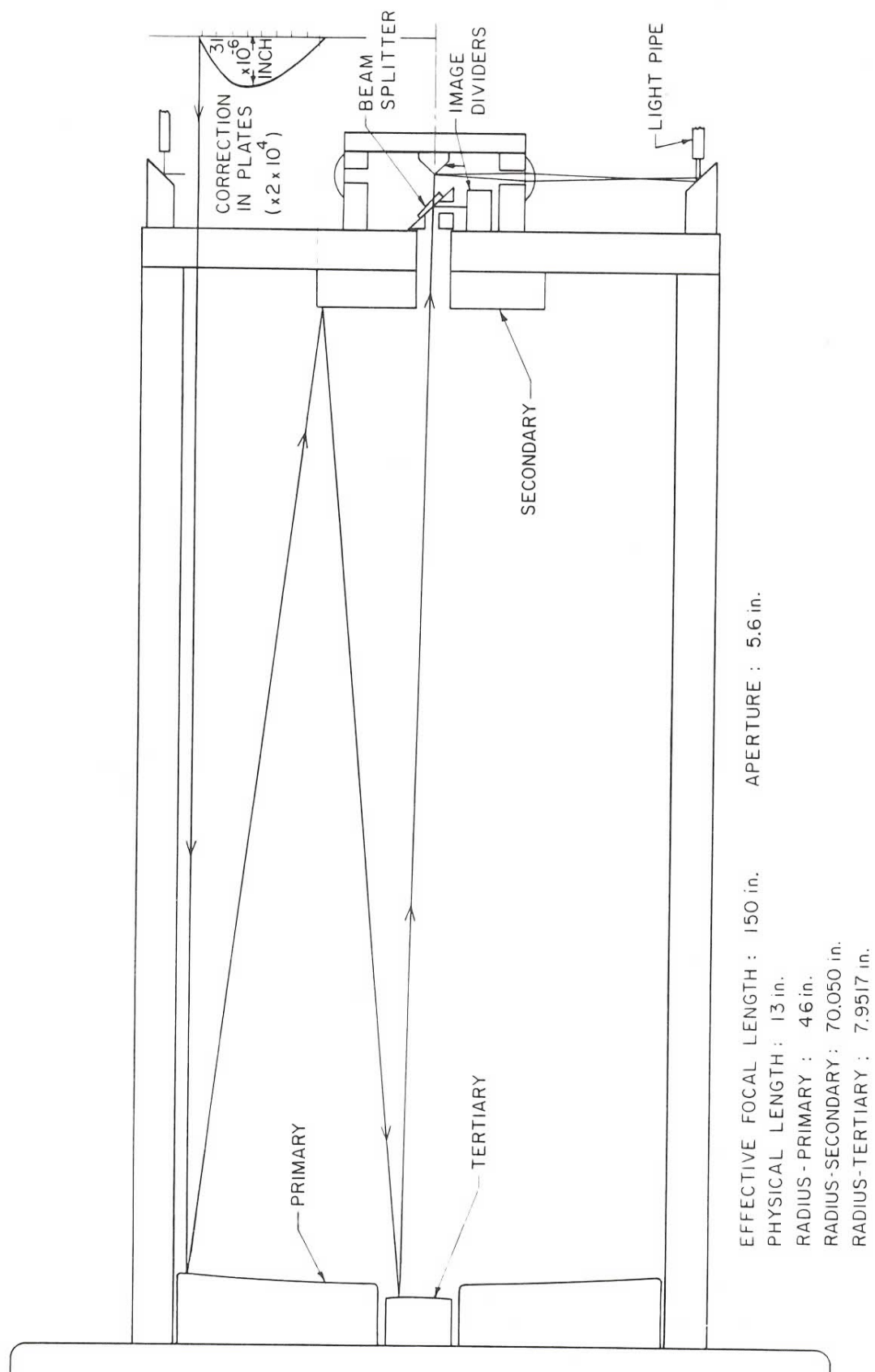


Figure 5
Ray Diagram of the Telescope

overall length 14 in. and outside diameter 7.5 in. The parts are made entirely of fused quartz and are held together by a method known as optical contacting, i.e., by direct molecular adhesion of the quartz surfaces. This method eliminates the use of cement or bolts and nuts.

Angular readout is obtained as follows. Located about an inch in front of the focal plane is a beam splitter which forms two star images, one for each readout axis. Each image then falls on the sharp edge of a roof prism where it is again subdivided into two half images. The angle between the line of sight to the star and the two readout plans are determined by measuring their relative intensities. The light beams are chopped by a mechanical chopper and the output of the photomultiplier is synchronously detected at the chopping frequency. This method singles out the relevant signals from drifts and instrument errors.

VIII. London Moment Readout

It is a challenge to determine the spin axis and its precession from a perfectly round and homogeneous rotor. Neither optical monitoring of a surface pattern nor extracting from the suspension signals components due to mass unbalance would work.

C.W.F. Everitt of Stanford suggested that the spin axis could be monitored from the London magnetic moment developed by making the gyro go superconducting. The London moment⁹ of a spinning sphere is given by

$$\vec{M}_L = \frac{mc}{e} r^3 \vec{\omega}_s$$

where r is the radius and $\vec{\omega}_s$ is the spin angular velocity of the sphere and $mc/e = 10^{-7}$ emu is the mass/charge ratio of the electron multiplied by the speed of light.

Fig.6 illustrates the principle of the readout. Surrounded by a superconducting pickup loop, any change in the gyro spin axis would result in the same vectoral change of \vec{M}_L . A cancelling current is then generated in the pickup loop and is proportional to the sine of the angle. A SQUID [Superconducting QUantum-mechanical Interference Device] magnetometer can be employed to measure this tiny change in magnetic field. Three orthogonal loops are necessary for a complete determination of the gyro orientation.

The readers are referred to reference 10 for more detailed discussion of the subject.

IX. Ultra Low Magnetic Field

The magnetic field environment allowed for the gyro is below 10^{-6} gauss in order to keep the relevant drift under 1 milliarc-sec. Another reason for an ultra-low field environment is due to the employment of SQUID to monitor the relativistic precessions. Too high a trapped field may drive the SQUID and/or its following amplifier into nonlinearity. The trapped field should be no more than 10^{-7} gauss and the sensitivity required to measure a gyro precession of 1 milliarc-sec/year is a few times 10^{-13} gauss.

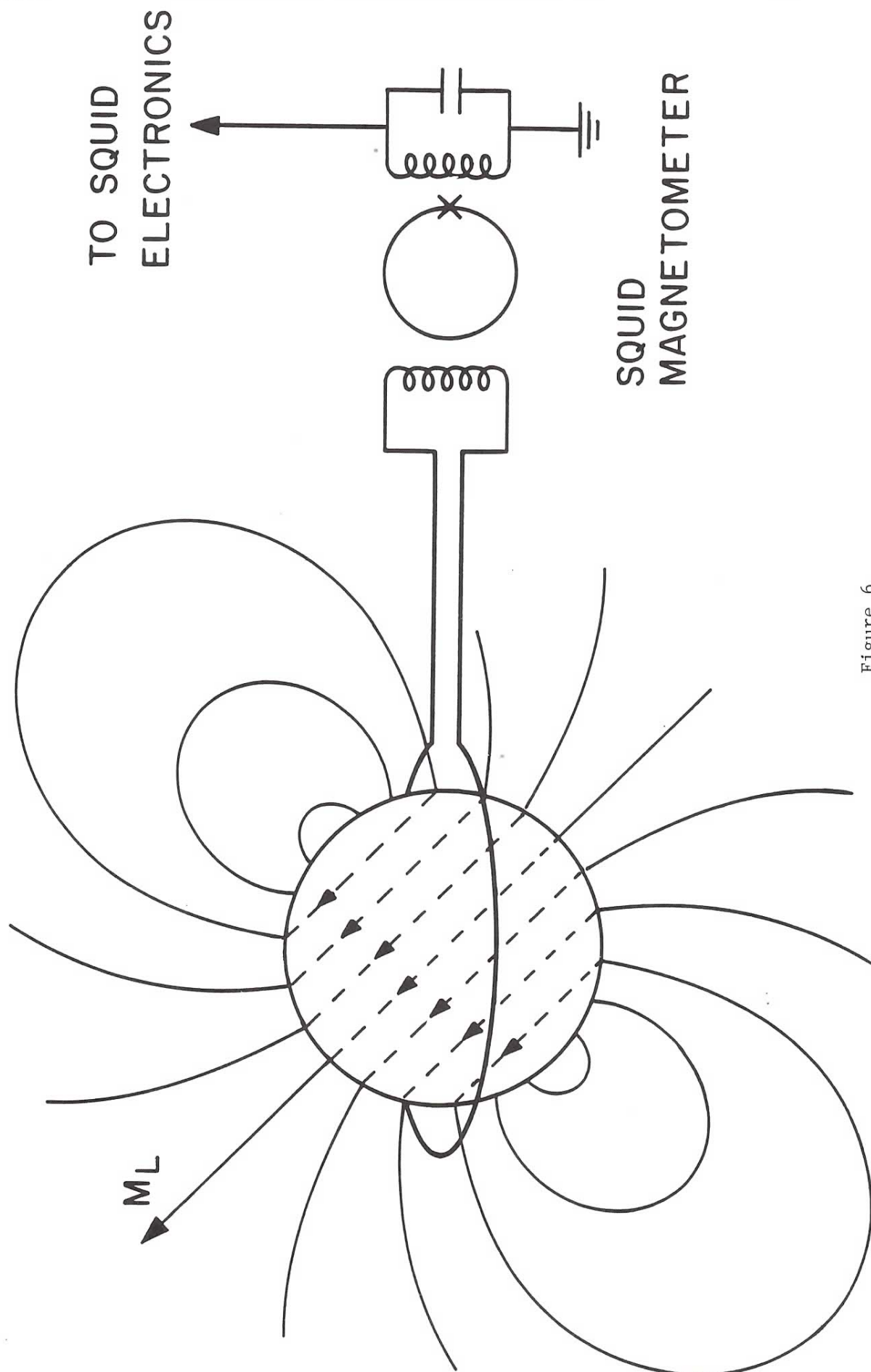


Figure 6
London Moment Readout

Low magnetic field environment are conventionally achieved by either using high permeability metal (passive method) or actively tune out the external fields. These methods yield a region of 10^{-5} gauss or slightly lower. For our purpose, a field stable over long periods of time to a few parts in 10^{-13} gauss is needed since any change in ambient field will disturb the readout. The only way is to take advantage of superconductivity and employ a superconducting shield.

The magnetic flux, $\phi = \vec{B} \cdot \vec{A}$, inside a superconducting loop is conserved. If the loop or a bag, initially compressed, is expanded, the increase in area is followed by a decrease in magnetic field.

Between 1969 and 1975, B. Cabrera¹¹ of Stanford developed a procedure for making 10^{-7} gauss shields. Fig.7 shows the cyclic procedure in which a lead bag is cooled and expanded inside another bag. After three to four cycles, starting with initial field about 10^{-5} gauss, a field of a few parts in 10^{-8} gauss can be achieved.

Another important factor in this ultra low field process is the choice of material inside the bag. The material must be non-magnetic and must not generate thermoelectric fields. Among materials studied by Cabrera, quartz is one of the best.

X. Error Analysis

In a separate talk in this conference, C.W.F. Everitt will give an extensive account on the error analysis of the Relativity program. We shall discuss this subject briefly here.

Table I lists the design requirements for a gyro that would yield a limiting drift rate of 0.3 milliarc-sec/year.

The out-of-roundness of the gyro would cause drifts when it is electrically suspended. Such drifts are due to interaction between local hills and valleys with the electrodes. Also, since the gyro is never a perfect sphere before and after the thin film deposition of the superconductor, the non-coincidence of the center of mass and the center of geometry gives rise to a mass-unbalance torque. None of these torques would be present if the gyro was a perfect sphere. However, these torques go down by many orders of magnitude when the gyro operation is moved from an earthbound laboratory to space; they are zero in an absolute zero-g environment.

A non-spherical gyro can be expressed in terms of Legendre polynomials. Suspension torques can then be viewed as interaction of the electrodes with each term. Conversely, similar torques exist if the gyro is perfectly round but the gyro housing is not. The sphericity requirement on the housing is partly to eliminate certain higher order suspension torques and partly to reduce torques due to local static charge build-up.

The expression of the motional precession suggests that the precession rate goes up with angular speed. That the gyro is not a rigid body

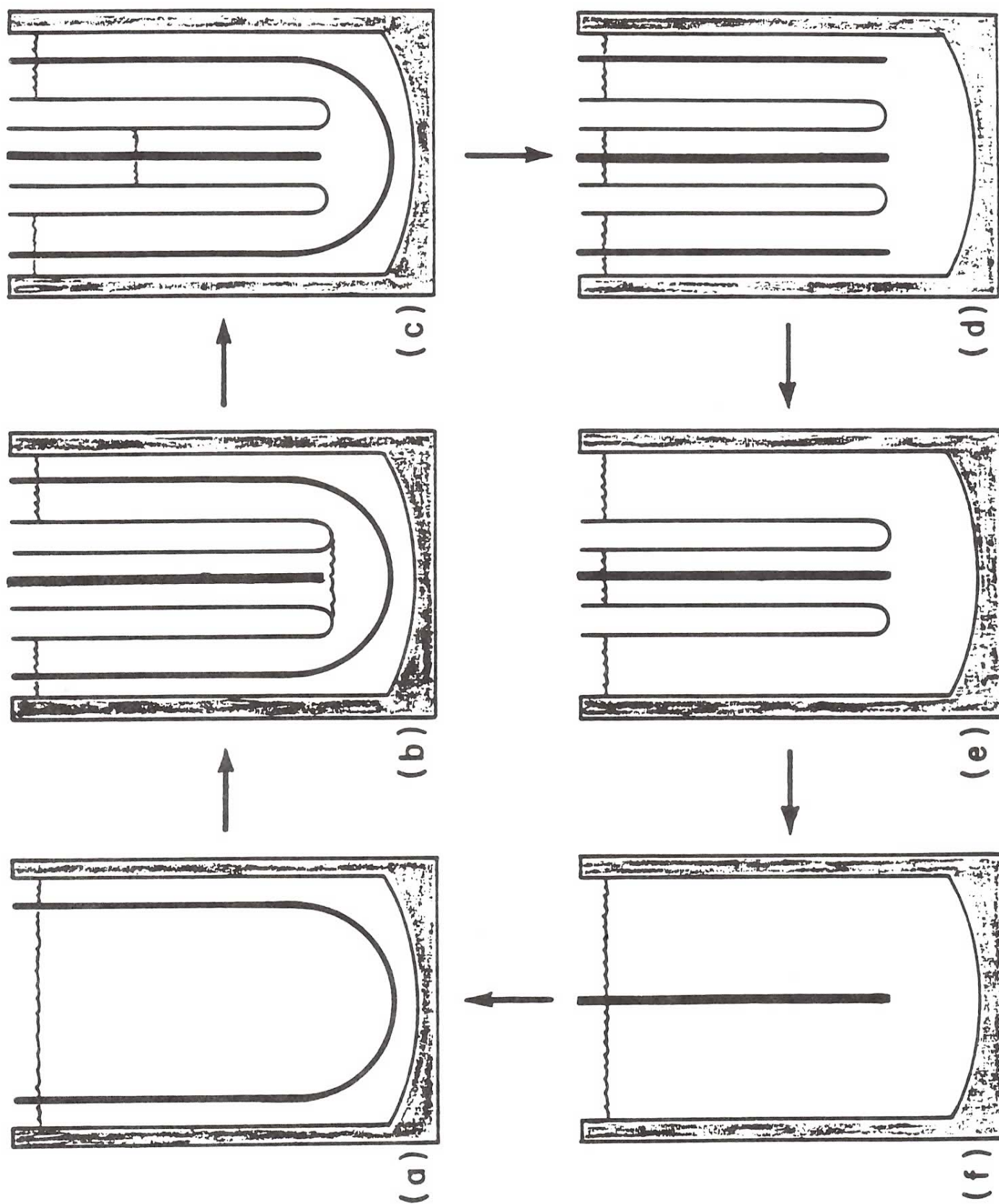


Figure 7: Cyclic coding and expansion of lead shields to create a region of ultra low magnetic field.

Design Goals for Gyro with Residual Drift-Rate below 0.3 milliarc-sec/year

	Goal	Achievement to Date
Rotor Homogeneity	3×10^{-7}	10^{-6}
Rotor Sphericity	0.8 μin	0.8 μin
Coating Uniformity	0.3 μin	$\left\{ \begin{array}{l} \text{best uniformity} \quad -2\% \\ \text{thinnest coating} \\ \text{levitated} \quad -9 \mu\text{in} \end{array} \right.$
Housing Sphericity	20 μin	8 μin
Centering Stability	7.5 μin	7.5 μin^*
Optimum Preload	0.2 V	-----
Optimum Spin Speed	170 Hz	110 Hz
Drag-Free Performance	10^{-10} g	5×10^{-12} g
Magnetic Field Level	10^{-7} G	2×10^{-8} G
Charge on Rotor	$< 3 \times 10^9$ electrons	$\left\{ \begin{array}{l} < 10^7 \text{ electrons}^\dagger \\ 10^{-7} \text{ torr with live gyro} \\ 2 \times 10^{-11} \text{ torr in low temperature} \end{array} \right.$
Pressure in Housing	10^{-9} torr	bakeout test

* Assumes temperature of electronics box controlled to $\pm 1.3^\circ\text{C}$ over roll cycle

† Estimate based on observed upper limit of charge for DISCOS proof mass

Table 1

limits the angular speed due to centrifugal distortion on the gyro. The optimum spin speed occurs at around 170 Hz.

Table II gives a summary of the calculated drift errors from various sources based on the design criteria listed in Table I.

XI. Data Acquisition

A proper instrumentation for the experiment should a) process and store the relativity data, b) provide signals for use in pointing and attitude control, and c) allow calibration of the telescope scale factor. The last item is necessary because the light intensity of the reference star changes over the year's course of solar system. The proposed design is largely due to R.A. Van Patten of Stanford and is illustrated in Fig.8. Drawn in heavy lines is an integrating data loop which supplies updated relativity data in digital form. This is the output of a precision summing amplifier Σ_1 which has three inputs - gyros' readouts, the telescope readout, and a return from a closed loop system explained as follows. The instantaneous output of Σ_1 is converted into DC by the demodulator. This DC voltage is then converted by the voltage-to-frequency device driving an up-down binary counter. The binary output contains the readout signal for storage and telemetry. At this point, the output represents the relativity data which is the difference between the gyro and the telescope readouts. The output is then converted into analog voltage by the D/A converted and fed back to the amplifier Σ_1 such that a null is now maintained at the Σ_1 output. The closed loop operation can be understood by the following algebra. Call the gyro output G, the telescope output T, and the signal in the up-down counter R. The output at the summing amplifier provides the function $(T-G+R)$. If the output is maintained at null, we have $R=G-T$, which is the relativity data.

The second summing amplifier Σ_2 gives control information of the pointing servos. In normal operation, Σ_2 gives the direct telescope error. If the spacecraft suffers from any external disturbances such as meteorite impact or occultation of the star by the earth, the telescope output is interrupted. The control logic stops T and the Σ_1 output can no longer be nulled and is instead G-R. By holding R fixed during the interruption, the spacecraft will still be pointing at the star with control coming from the gyroscope output. Note that R is not the accumulated relativity data; rather it is the relativity data right before the interruption. When the telescope data are resumed, the reverse counter will run until the instrument loop has been driven to null. Hence, there is a small loss of relativity data collection as a result of the interruption.

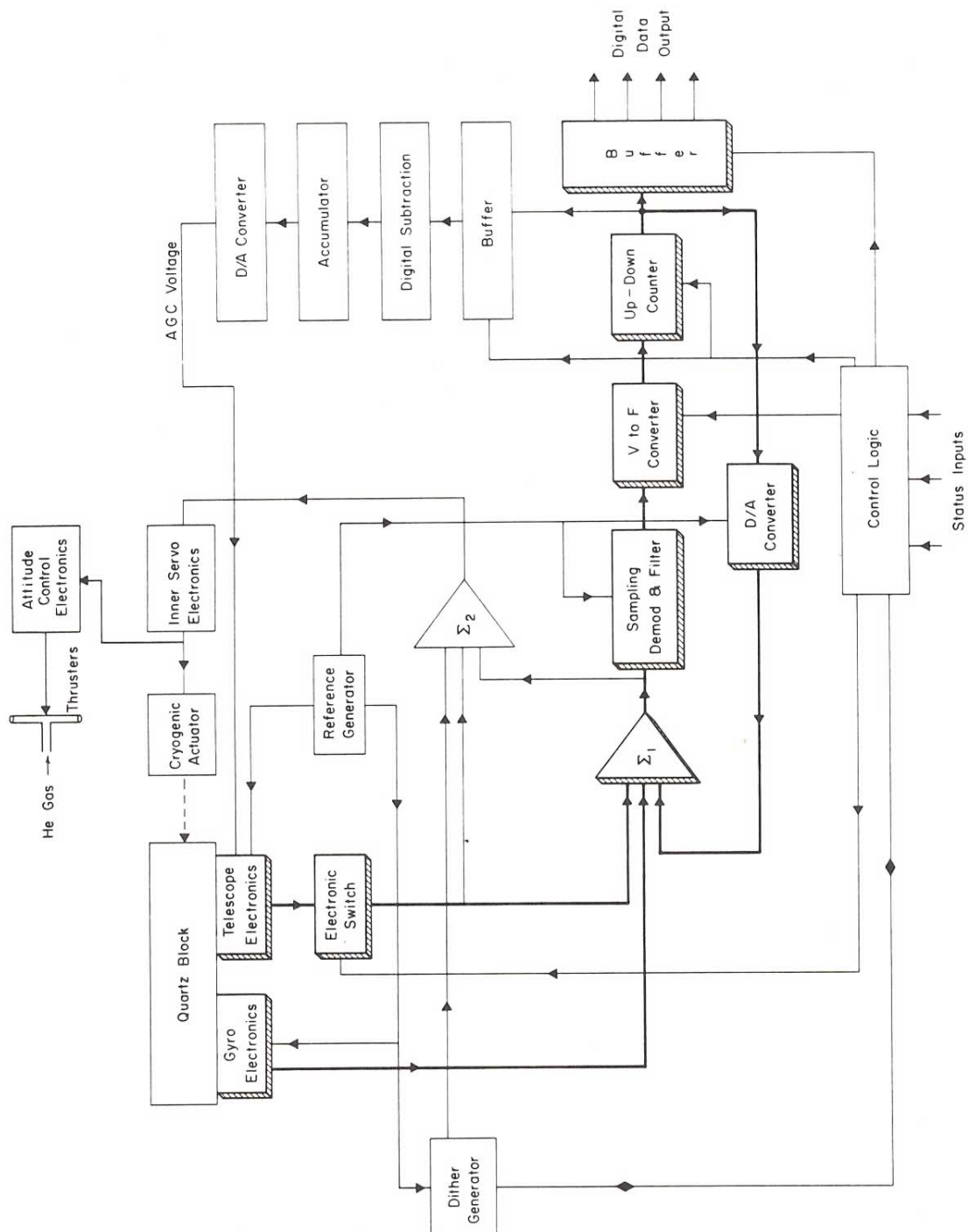
The telescope scale factor is calibrated in the following manner. A low frequency dithering signal introduced to the inner servo loop which controls the fine mechanical motion of the telescope-gyro housing assembly relative to the dewar, i.e., the spacecraft, by means of actuators which may be piezoelectric crystals. As a result, the assembly sway back and forth through a small angle about the line of sight of the star. The dithering frequency is about 0.1 Hz. A signal output appears at the instrument loop if the scale factors of the two readouts are not

Class	Type	Assumption	Drift-rate (milliarc-sec/year)
Support independent			
Electric	Static charge on rotor	static voltage less than 0.15 V preload	< 0.001
	Patch effect	10^3 patches with $v_c \sim 0.2$ V	< 0.011
Magnetic	From readout rings		
	• readout reaction	readout feedback gain of 10^4 below 1 Hz	< 8×10^{-6}
	• differential damping of trapped flux	readout feedback unity gain frequency of 10 kHz	< 10^{-14}
	From superconducting shield		
	• trapped flux	10^{-7} gauss in shield	$\sim 10^{-4}$
	• hole in shield	1.1 cm dia. hole	< 2×10^{-4}
	From superconducting electrodes		
	• reaction pressure	10^{-7} gauss in electrodes	< 2×10^{-4}
	• trapped flux	0.15 V preload, 10 min. roll rate	< 0.002
	From rotating electric support field		< 2×10^{-10}
Gas	Differential damping	6 per cent variation over electrodes, 10^{-9} torr pressure	< 0.15
	Roll induced torque	10 min. roll rate, 10^{-9} torr pressure	< 0.04
Random walk effects	Brownian motion	10^{-9} torr pressure	$\sim 2 \times 10^{-4}$
	Photon bombardment	$T \sim 1.6$ K	< 10^{-6}
Effects of cosmic rays	Primary		
	• protons		< 2×10^{-5}
	• iron nuclei		< 10^{-3}
	South Atlantic anomaly		4×10^{-4}
	Showers from Sun		4×10^{-4}

W.S. CHEUNG

1983

Table 2
Error Sources



RELATIVITY INSTRUMENTATION SYSTEM

Figure 8

equal. Such a difference in scale factor is then corrected by means of first synchronously detecting the difference at the dither frequency and then followed by an automatic gain control sequence.

The spacecraft is also made to roll about the line of sight of the star at a period of about 10 minutes. The rolling motion in effect chops the gyro reading at the roll-rate. Again, synchronous detection at the roll frequency can single out the gyro reading in the presence of $1/f$ SQUID noise; other instrument effects can also be averaged out by the rolling.

XII. Electrical Breakdown Study

The problem of electrical breakdown comes in when the gyro is levitated and studied on Earth. Even in a perfect vacuum, cold electron emission still occurs across two electrodes under high voltage difference. The electric pressure literally pulls electrons out of the cathode. The emission becomes more acute at regions of microscopic hills and valleys where the local electric field intensity is enhanced by a factor typically between 10 to 100. The sharp points act like lightning rods and are believed to be responsible for the arcings observed occasionally during gyro levitation. Ionization of residual gas of an ordinary vacuum and the presence of impurities in the electrodes often trigger early arcings.

Arcings, however, tend to level off a local point. This is known as burn-in. A gyro with thick coating, 100 μ in to 1 mil, can generally survive these arcings. Experiences at Stanford with thin film gyros, 1 to 10 μ in, indicate otherwise and rupture of a thin film sometimes results.

J. Lipa of Stanford began a study of vacuum electrical breakdown phenomenon for bulk and thin film materials. After several modifications, the present setup, which is still rather crude, is shown in Fig.9. Observations so far indicate that thin films follow a different breakdown pattern as compared to bulk materials. This setup is currently being automated.

A rotor acceptance scheme has been conceived by Lipa and this author and is shown in Fig.10. The emission current patterns of a given coated gyro can be mapped with the aid of a computer. The computer can also direct a burn-in procedure at areas where high emission currents are observed. Information so obtained can be interpreted as the rotor's tolerance, when electrically suspended on Earth or in space, against external accelerations.

Acknowledgement:

This work is supported by a NASA contract NAS8-34619. The author wishes to thank the following members of the Stanford group, principal investigators and investigators alike, for their support and technical assistance: J.T. Anderson, J. Bourg, J. Breakwell, B. Cabrera, R.H. Cannon, D. DeBra, C.W.F. Everitt, W.M. Fairbank, R. Farnsworth, J. Gill, G.M. Keiser, P. Levine, J. Lipa, J. Lockhart, J. Turneure, and R.A. Van Patten.

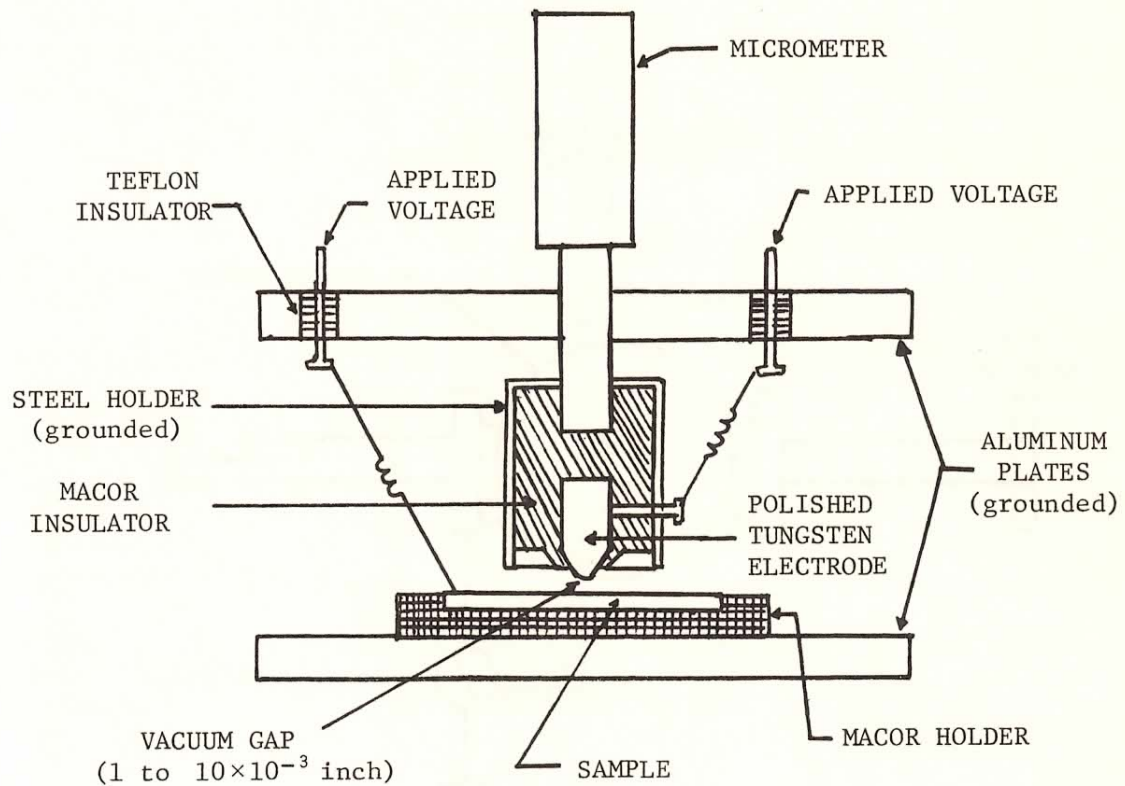


Fig. 9. A simple setup to study electrical breakdown behavior of thin films. The micrometer adjusts the gap between the tungsten electrode and the sample. The assembly is housed inside a vacuum can that is maintained at 10^{-6} torr.

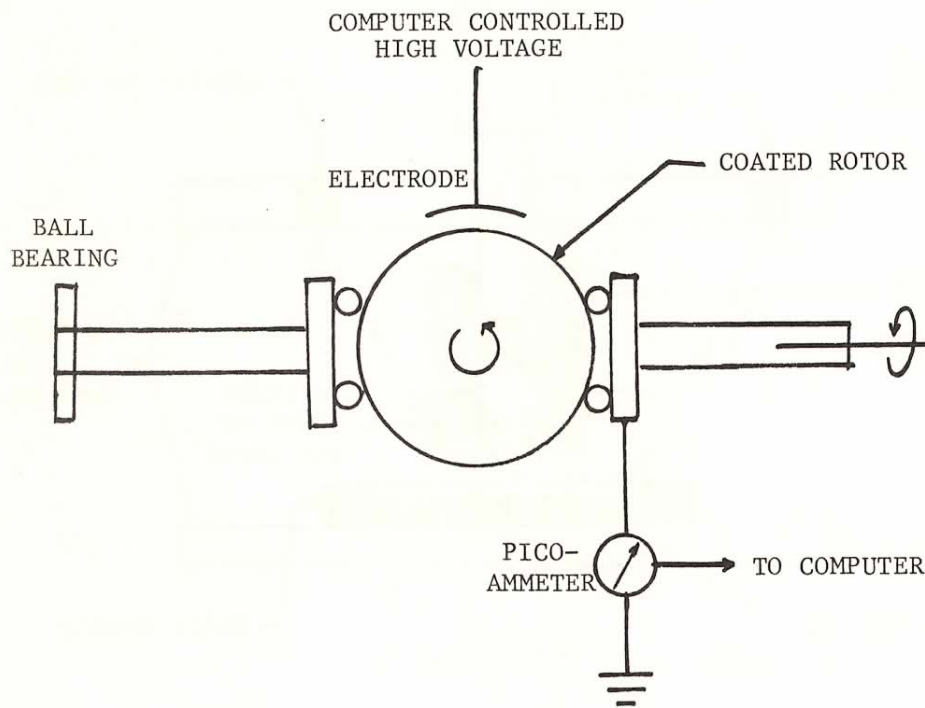


Fig. 10. A conceived scheme of rotor-acceptance program. The coated rotor can be tumbled along two axes. A computer controlled high voltage is applied at the electrode and the emission current at each covered area is recorded. The emission current characteristics of the rotor can then be mapped out.

References

1. A thorough presentation can be found in an article by C.M. Will, General Relativity, an Einstein Centenary Survey, ed. S.W. Hawking and W. Israel (Cambridge Univ. Press, N.Y., 1979), pp.24.
2. R.V. Pound and G.A. Rebka, Jr., *Phys. Rev. Letters*, 4, 337 (1960).
3. L.I. Schiff, *Proc. Nat. Acad. Sci.*, 46, 871 (1960).
4. C. Brans and R.H. Dicke, *Phys. Rev.* 124, 925 (1961).
5. J. Lense and H. Thirring, *Phys. Zeits.* 19, 156 (1918).
6. G.J. Siddall, "Refractive Index and Density Relationship For Fused Quartz" (Stanford University Memorandum, W.W. Hansen Labs. of Physics, Stanford, May 1979).
7. W. Angele, *Prec. Eng.*, 2, 119 (1980).
8. J.T. Anderson, et. al., Proceedings of the Second Marcel Grossmann Meeting on General Relativity, ed. R. Ruffini (Amsterdam, North Holland, 1982), Part B, pp.939-957.
9. F. London, Superfluids, Vol.1: Macroscopic Theory of Superconductivity (Wiley, 1950), pp.78-82.
10. J.A. Lipa, et. al., Low Temperature Physics LT-14, ed. M. Crussius and M. Vuorio, Vol.4 (Amsterdam, North Holland, 1975).
11. B. Cabrera, Ph.D. Thesis, Stanford University (1975).